STRUCTURE OF CORTICAL MICROTUBULE ARRAYS IN PLANT CELLS

A. R. HARDHAM and B. E. S. GUNNING

From the Department of Developmental Biology, Research School of Biological Sciences, Australian National University, Canberra, A.C.T. 2601, Australia

ABSTRACT

Serial sectioning was used to track the position and measure the lengths of cortical microtubules in glutaraldehyde-osmium tetroxide-fixed root tip cells. Microtubules lying against the longitudinal walls during interphase, those overlying developing xylem thickenings, and those in pre-prophase bands are oriented circumferentially but on average are only about one-eighth of the cell circumference in length, i.e., 2–4 μm. The arrays consist of overlapping component microtubules, interconnected by cross bridges where they are grouped and also connected to the plasma membrane. Microtubule lengths vary greatly in any given array, but the probability that any pass right around the cell is extremely low. The majority of the microtubule terminations lie in statistically random positions in the arrays, but nonrandomness in the form of groups of terminations and terminations in short lines parallel to the axis of cell elongation has been observed. Low temperature induces microtubule shortening and increases the frequency of C-shaped terminations over the 1.7% found under normal conditions; colchicine and high pressures produce abnormally large proportions of very short microtubules amongst those that survive the treatments. Deuterium oxide (D_2O) treatment probably induces the formation of additional microtubules as distinct from increasing the length of those already present. The distribution of C-shaped terminations provides evidence for at least local polarity in the arrays. The validity of the findings is discussed, along with implications for the development, maintenance, and orientation of the arrays and their possible relationship to the orientation of cellulose deposition.

KEY WORDS microtubules · plant cell cortex · pre-prophase bands · xylem · serial sectioning

The discovery of cortical microtubules in plant cells followed the introduction of glutaraldehyde as a fixative for fine structural studies. Ledbetter and Porter (28) described them as being "arranged circumferentially [against the lateral walls of root tip cells] . . . like hundreds of hoops around the cell," parallel to microfibrils of cellulose in the cell wall. While admitting that individual microtubules could be followed for only short distances, Newcomb (34) stated that "In some cases they run circumferentially around the cell in the cytoplasm near the plasmalemma, probably forming complete rings or hoops." Green *et al.* (13) also considered that cortical "microtubules are arranged in a very loose spiral or are present as rings." Srivastava and Singh's description (53) of microtubules overlying developing xylem thickenings is that they too "run like hoops around the cell," and Hepler and Palevitz (21) refer to those

in a differentiating sieve element as being "arranged hooplike around the cell." Even more recently, Pickett-Heaps (41) envisaged that "cytoplasmic microtubules normally encircle the cell transversely to the long axis in both higher plants and many algae." Schnepf *et al.* also implied that the cortical microtubules are long in suggesting "unusually fast elongation of the microtubules [along a newly formed wall] so that they soon appear on the opposite wall . . ." (48).

There is, however, growing evidence that microtubular arrays can contain overlapping rather than full-length microtubules (11, 18, 20, 23, 26, 32, 33, 59). In the case of the plant cell cortex, this might be of especial importance. It has become evident that the congruent alignment of cortical microtubules and wall microfibrils is widespread during primary and secondary wall deposition (21), and any attempt to specify functional aspects of this co-orientation is crucially dependent upon knowledge of the actual three-dimensional arrangement of the microtubules. At least one hypothesis views the microtubules as providing rigid guide tracks for the movement of cellulose synthetase complexes (19). Yet, there is in fact no compelling evidence that cortical microtubules are long hoops or helices. Warnings given by the original discoverers that they could equally be in the form of overlapping arcs (27, 29) have gone largely unheeded. The main aim of the present work was to provide basic information on the geometry of cortical microtubule arrays in plant cells, this being fundamental to an understanding of how they are formed and maintained, and how they might function. Preliminary data have been published (16, 17).

MATERIALS AND METHODS

Plant Tissue and Routine Fixation

Root tips of *Azolla pinnata* R.Br. (comprehensive descriptions in preparation), *Impatiens balsamina* L. and *Zea mays* L. were fixed in 2.5% glutaraldehyde in 0.025 M phosphate buffer, pH 7, for 2–17 h at room temperature, rinsed in buffer, and postfixed in 2% osmium tetroxide in the same buffer for 2 h at room temperature. The tissue was dehydrated in graded acetone solutions and embedded in Spurr's resin (52). Variations from this standard procedure are described in Table I and appropriate parts of Results.

Experimental Treatments

For low temperature treatments, intact *Azolla pinnata* plants were transferred to culture medium in beakers surrounded by ice in a cold room, for either 15 min or 4 h. The temperature of the water in which the roots were immersed varied within the range 0°–2°C in different experiments (Table VI). Roots were fixed for 1 h at this temperature and then for a further hour at room temperature. In a recovery experiment, roots were transferred to room temperature culture medium for 15 min before fixation at room temperature. The rate of cooling and warming in the actual root tissue was not measured, but since the diameter of the root at the level that was analyzed is only ~150 μm, it is assumed to be rapid. Treatments with colchicine in the dark at 5×10^{-3} M lasted 2, 3, 4, or 5 h, as well as 2-h treatment followed by a 1-h recovery. Deuterium oxide (D_2O) was used at 99.8% purity for 5 or 18 h before fixation (in glutaraldehyde dissolved in D_2O). Pressures of 6,000 lb/in^2 (for 30 min), 14,000, or 16,000 lb/in^2 (for 15 min) were applied to intact *Azolla pinnata* plants, using a French pressure cell. The pressure was released smoothly but quickly, and roots were immersed in fixative within 30 s of the onset of decompression.

Serial Sectioning

Ribbons of sections cut from longitudinally oriented roots were collected on parlodion-coated grids with 2-mm slots and stained with saturated uranyl acetate in 50% ethanol for 30 min, then in lead citrate for 10 min (56), and viewed in a Hitachi H500 electron microscope. Suitable preparations were photographed at × 30,000 and printed to a final magnification of 75,000.

Tracing and Mapping

Microtubule profiles were traced from the micrographs of each serial section onto cellulose acetate sheets. Individual microtubules were followed by placing the tracing of one section over the micrograph of the adjacent section in the sequence. When the entire sequence had been analyzed in this way and the positions of terminations and the paths of the microtubules determined, the position of each microtubule profile on the tracings was plotted on graph paper so as to build up a map of the tubules in the plane of the array (e.g. Figs. 4–6). Terminations were arbitrarily taken to occur halfway through the section in which they had been detected. Where possible, a microtubule which continued right through the sequence was used as a reference and each successive section was aligned with respect to it. Spatial separation of microtubules in the direction from the wall to the center of the cell cannot be depicted on these maps, and some microtubules which appear to lie very close together may, in fact, be some distance apart. In preparing the maps of some very dense arrays, it was necessary for the sake of clarity to displace the positions of a few microtubules just enough to show their existence.

Estimation of Section Thickness

The construction of the microtubule maps described above and the calculation of microtubule lengths is

dependent on knowledge of the section thickness. Ideally, the thickness of every section should be measured, so that variation such as is evident in Fig. 3 could be taken into account. We have adopted a compromise procedure, calibrating our ultramicrotome by estimating the depth to which ribbons of ultrathin sections of various interference colors cut into the block. Details are given in reference 15. An average section increment of 70 nm was estimated for the ribbons of serial sections used in the present work (this is a slight revision of the value given in reference 17).

Derivation of the Average Microtubule Length

Consider the microtubules to be arcs lying adjacent to the walls of a cylindrical cell, perimeter A, as viewed in transverse section in Fig. 1. The average length of the microtubule arcs, L, is assumed to be less than A. The cell is sectioned longitudinally and the total thickness of the combined serial sections is the sample arc, a. The lengths are assumed to be independent of position and of each other, the midpoints of the microtubules forming a poisson process of intensity, λ. In this situation, the expected number of terminations (T) occurring in the sample arc is given by $T = 2\lambda a$. The expected number of microtubules (N) passing through a fixed point is $N = \lambda L$, and hence the average microtubule length can be calculated from the relationship $L = 2Na/T$. An intuitive derivation is given in Results, and the validity of the formula is easily checked using imaginary arrays drawn on graph paper. The use of sections of finite thickness introduces an error which can be avoided if, when counting the number of profiles of microtubules per section in order to derive N (the average number per section), one unit is added for each tubule that is not terminating, and one-half unit for each tubule that terminates in that given section. Thus, it is assumed that the terminations always lie at the midplane of the sections.

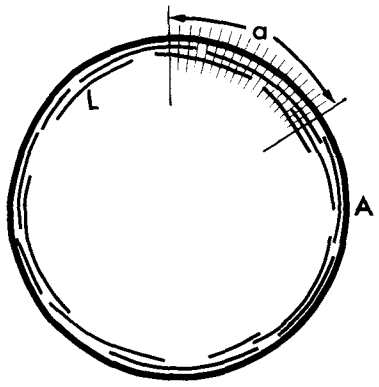

FIGURE 1 Microtubules, length L, lie adjacent to the perimeter of a cell, circumference, A. The sample arc, a, is equal to the thickness of the combined serial sections.

Analysis of the Spatial Distribution of Terminations

Objective methods for detecting possible nonrandomness in the distribution of terminations were applied. A multiple χ^2 test was used to compare the observed distribution of terminations amongst the sections in each sequence with that predicted by a poisson distribution calculated using the average number of terminations per section as its mean. The significance of calculated values of χ^2 was determined from the table given in reference 10. All of the arrays described in Results as "random" had probabilities of correspondence with poisson distributions $>P = 0.05$ (mostly $\gg$), and of those described as "nonrandom" the probabilities of correspondence were $\leq P = 0.01 - 0.02$ (mostly $\ll P = 0.01$). This analysis, however, indicates deviation from randomness only if the nonrandomly distributed terminations lie in a pattern that is detectable by the sampling procedure, i.e., by the cutting of sections in a particular plane. Evidence for nonrandomness due to clumping of terminations over several successive sections, or to lines of terminations not lying in the plane of the section, may be obtained by applying a pattern analysis which measures the variability or spread of a distribution of points (14, 24). In this procedure, a microtubule map is subdivided by a grid to give convenient grid units or "blocks," and the number of terminations in each block is counted. If their distribution is random the variance is equal to the mean, whereas larger values of variance indicate clustering, and lower values, regular dispersion. The variance of the population is calculated at different unit block sizes. The ratio of variance to mean is plotted against size, and confidence bands (55) are applied to determine sizes at which the distribution deviates significantly ($P = 0.05$) from randomness.

RESULTS

Microtubule Terminations in Longitudinal and Transverse Views

If an ultrathin section is 75 nm (i.e. three microtubule diameters) thick, any microtubule whose long axis deviates from the plane of section by as little as 4° will only have, at most, 1 μm of its length included within the section. The zone over which the microtubule leaves (or enters) the surface of the section will show a gradual loss of image of the tubule; Fig. 2*a* and *b*, which show two adjacent serial sections through a pre-prophase band of microtubules, contain many examples. In theory, it should be possible to follow microtubules in longitudinal view from one section

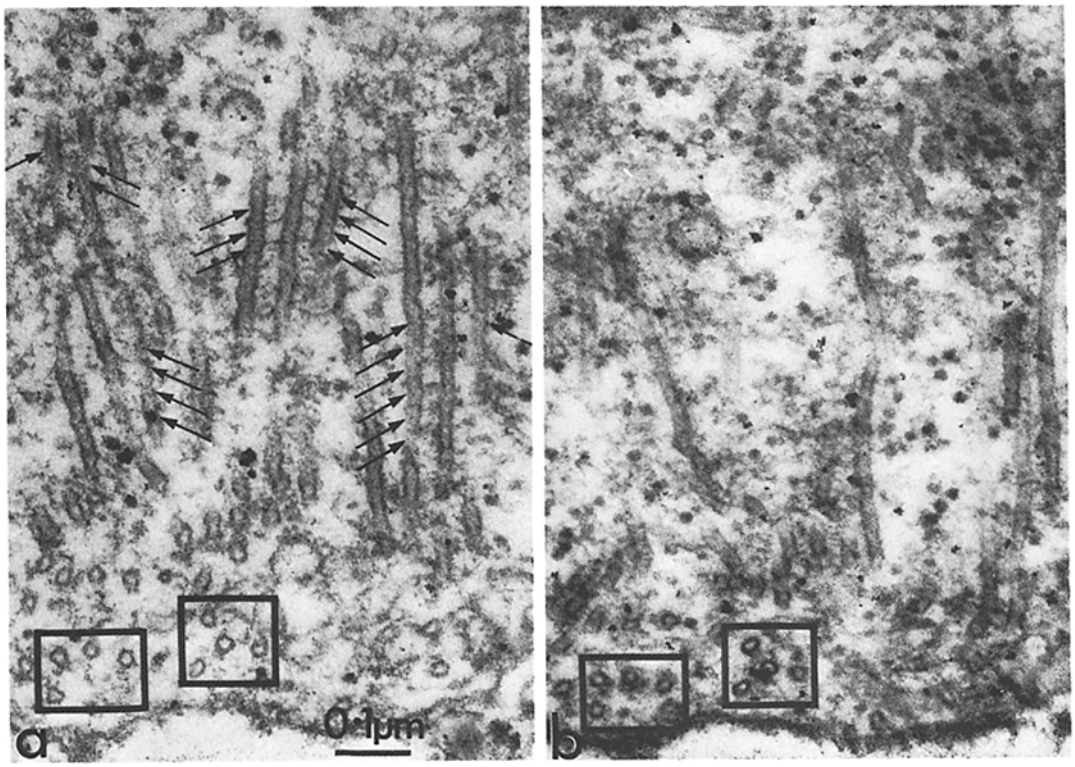

FIGURE 2 Two adjacent serial sections through a pre-prophase band of microtubules in an *Azolla* root tip cell illustrate the difficulty of tracking microtubules in longitudinal section. Microtubules that have been sectioned transversely can, however, be followed from one section into the next (see boxes). Periodic bridging between adjacent longitudinally sectioned microtubules is evident in Fig. 2*a* (arrows). × 100,000.

to another until terminations are found. In practice, it is very difficult to do so, especially in dense arrays of microtubules. However, where the microtubules lie at right angles to the plane of section, the relative positions of the circular transverse sectional profiles allow the presence or absence of a particular microtubule to be determined with confidence (Fig. 2*a* and *b*).

Examples of microtubule terminations can be seen by following the numbered microtubules in Fig. 3. 18 of the 42 microtubules that are present in this part of the sequence end within the sections shown, the terminations occurring throughout the array. The sequence includes one short complete microtubule which begins in Fig. 3*c* and ends in Fig. 3*j*.

No electron-dense material was consistently seen at termination sites, but 1.7% of the terminations were found to possess a C-shaped profile in transverse section (see Table V), as exemplified by microtubule number *2* in Fig. 3*a*. This conformation usually occurs in the last one or two sections but has been seen for up to 14 sections (1 μm) from the end of the microtubule. On two occasions, microtubules were found to possess C-shaped profiles which were isolated from the terminations by complete, circular profiles. Sometimes the arms of the "C" are much reduced, leaving only a small arc of the original microtubule profile.

The 12 C-shaped terminations (1.7% of a total of 706) showed nonrandom distribution patterns within the arrays. They were present in just three of the sequences of serial sections (all from different cells), one having two and the others four and six, respectively. C-shapes were never found at both ends of an individual microtubule, and if one mentally symbolizes a C-shape as an arrowhead at one end of a microtubule, then, in the array that had two C-shapes, both "arrows" pointed in the same direction. In the array with four C-shapes, all four pointed in the same direc-

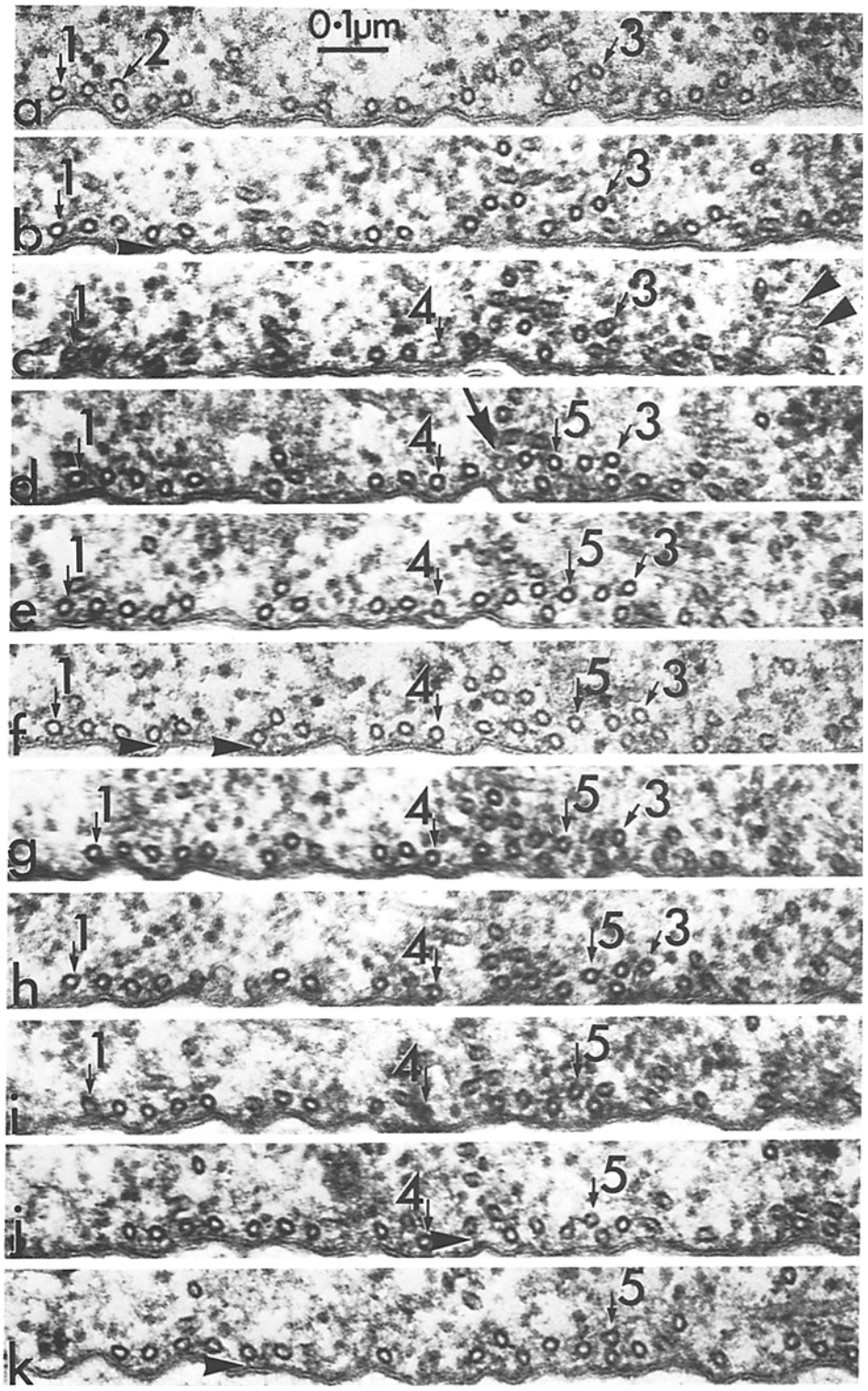

FIGURE 3 Eleven serial sections (*a–k*) through a pre-prophase band of microtubules in a root tip cell of *Azolla*. 18 of the 42 microtubules in this part of the array terminate within these sections. Examples of microtubule terminations can be seen by following the selected numbered microtubules: microtubules numbered *1* and *3* make their last appearances in Fig. 3*i* and *h*, respectively; microtubule 5 makes its first appearance in Fig. 3*d*. A C-shaped termination is illustrated by microtubule *2* in Fig. 3*a*. A microtubule containing a zone in which the staining is much fainter than in adjacent regions is arrowed in Fig. 3*d*. The entire length of microtubule *4* is encompassed within these 11 sections. Microtubules passing at a greater angle than the majority in the array, e.g. those in Fig. 3*c* (arrowheads), were not included in the mapping or calculations. Note bridges between microtubules and the plasma membrane (horizontal arrowheads). × 106,000.

tion, and the same applied to the array with six C-shapes. Within a given array, the microtubules with C-shaped terminations evidently share a common directionality, at least within the portions of the arrays encompassed in the sequences of serial sections.

Bridges

Several examples of cross bridges between adjacent microtubules and also between microtubules and the plasma membrane are illustrated in Figs. 2 and 3. The bridging between the longitudinally sectioned microtubules in Fig. 2*a* exhibits a herringbone pattern with a periodicity approximating to the diameter of the microtubules themselves. Bridges attached to transversely sectioned microtubules are not readily distinguished from other material that may be lying close to the microtubules. However, relatively clear images of putative bridges were seen in all three categories of cortical array: in pre-prophase bands (Figs. 2 and 3), in interphase arrays, and in arrays of microtubules overlying developing xylem thickenings. They are present on short as well as long microtubules. In a number of cases, a cross bridge either to the plasma membrane or to an adjacent microtubule occurred on the terminating profile of a microtubule. On occasions, two bridges connected a single microtubule profile to the plasma membrane. Cross bridges between microtubules in pre-prophase bands and vesicles were occasionally seen.

Treatments which are known to stabilize microtubules or which can cause their depolymerization were used in parts of this study (see later): following all such treatments, the appearance and distribution of the microtubule cross bridges were similar to those described above in control tissues.

Microtubule Maps

It is evident from the microtubule maps (Figs. 4–6) that, in all three types of cortical microtubule array described below, some microtubules continue right through the sequence, others have one end within the sequence, and a few have both ends in the sequence, that is, the complete microtubules lie within the thickness of tissue sectioned. Many neighboring microtubules maintain the same relative spacing within small bundles over long distances (Fig. 6), but some show undulations. Some (usually lying deeper in the cytoplasm) pass at an angle to the remainder, and some leave one bundle and slant across to join another bundle. There is a tendency for isolated tubules to have atypical orientations. Microtubules lying at large angles to the majority were occasionally seen in the sequences of sections, e.g. Fig. 3, but were not included in the maps or calculations.

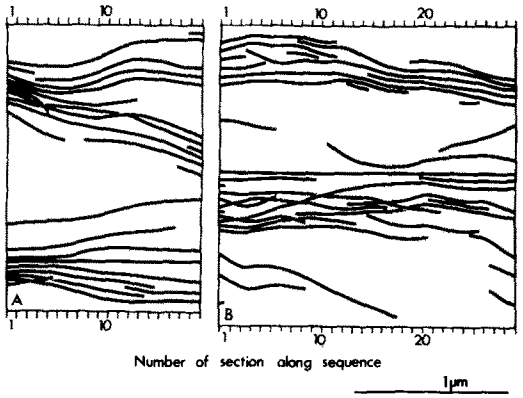

FIGURE 4 Two reconstructions of arrays of microtubules in developing xylem elements. In Fig. 4 A the microtubules were grouped over two clearly discernible wall thickenings at the beginnings of the sequence; however, by section 8 the thickenings were no longer visible. The reconstruction shows that in this region the microtubules begin to fan out, becoming more evenly distributed over the plasma membrane. Fig. 4 B depicts an array overlying two thickenings in material that had been treated with D_2O for 5 h. The thickenings were more developed than those in Fig. 4 A and continued throughout the sequence of sections. In these maps, as in all others except Fig. 6 A, the arrays are viewed as from the cell wall looking into the cell through the plasma membrane.

DIFFERENTIATING XYLEM ELEMENTS: An early correlate of the initiation of wall thickenings in developing xylem is the appearance of groups of microtubules along the longitudinal walls (39, 40). In studying the development of xylem elements in *Azolla pinnata* roots, it was often observed that microtubules were grouped on one side of the cell while they were distributed more evenly along the opposite wall. One reconstruction of a microtubule array in a xylem element followed the convergence from a dispersed array to a pattern of groups, visible wall thickening commencing where the groups are clearly established (Fig. 4 A). In reconstructions of other elements, the microtubules remained grouped over thickenings throughout the sequences.

PRE-PROPHASE BANDS: Pre-prophase

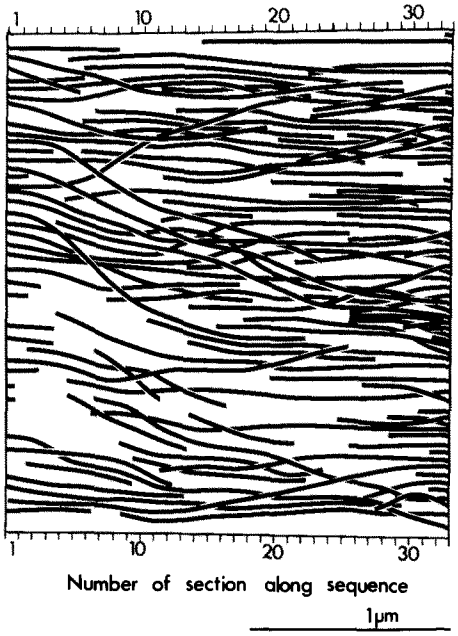

FIGURE 5 A reconstruction of part of a pre-prophase band of microtubules. The dimension normal to the cell surface is not apparent, but only 57–72% of the microtubules were adjacent to the plasma membrane. Most microtubules lie parallel to the plasma membrane, and are not interwoven.

bands of microtubules (41) occur throughout *Azolla* root tips, encircling the cells and anticipating the plane of every category of cell division (details in preparation). The number of microtubule profiles in a band varies widely, from 30 to >100. Where the number is small, most lie close to the plasma membrane; where it is large, the width of the band remains ~2 μm and the microtubules become stacked. The number can change (Fig. 5), sometimes markedly (Fig. 8), within a short sequence of sections. In the five pre-prophase bands that were serially sectioned, between 48 and 74% of the microtubule terminations occurred near the plasma membrane. In general, this percentage approximates to the percentage of microtubules that lie adjacent to the plasma membrane. Further analysis of the positions of terminations in pre-prophase arrays shows that, for 90% of the microtubules that were completely included in the sequences of sections, both terminations of any given microtubule lay at the same distance from the plasma membrane.

INTERPHASE ARRAYS: As in differentiating xylem elements, and in pre-prophase bands, the numbers of microtubules on opposite sides of an interphase cell are not always equal. While in most sequences of serial sections the numbers of microtubule profiles per section remained relatively constant (e.g. Fig. 6 A), a few cases were found where they slowly changed (e.g. Fig. 2 in reference 17). The array shown in Fig. 6 B includes a very abrupt change. In this case, 11 of the 13 microtubules in section 24 terminated and only two continued into section 22. As the sequence continued, the number of microtubules slowly increased again. Fig. 6 A contains a less obvious line of terminations at the same part of the sequence, the two arrays in Fig. 6 lying back to back, <1 μm apart in adjacent interphase cells.

Analysis of the Distributions of Microtubule Terminations

The observed distribution of microtubule terminations throughout the sequences of sections was compared to theoretical distributions calculated for each sequence from poisson series in which the mean is the number of terminations per section. In the majority of cases obtained from untreated root tips, the observed dispersion of terminations did not differ significantly from the poisson distributions, but in three interphase arrays and one pre-prophase band deviation from randomness occurred, due to the presence of either (*a*) clusters of terminations where most of the members of a parallel group ended within a few sections (as in two interphase arrays, e.g. Fig. 2 in reference 17) or (*b*) linear arrangements of terminations (as seen in the interphase array in Fig. 6 B and in the pre-prophase band). Other linear arrangements of terminations were seen, but since the line did not coincide exactly with the plane of sectioning, the overall agreement with the poisson distribution was retained. Similarly, some microtubule maps gave visual impressions of clustering but because the terminations, although clustered, were dispersed amongst several sections, the overall distribution did not deviate significantly from the poisson series.

A pattern analysis which can show whether a set of points is randomly distributed, clustered, or regularly dispersed was also used. When applied to the microtubule arrays, significant clustering of terminations was found to occur in all of the sequences which had, and three sequences which had not, deviated from the poisson distribution. Thus, in seven of the 16 arrays analyzed in this

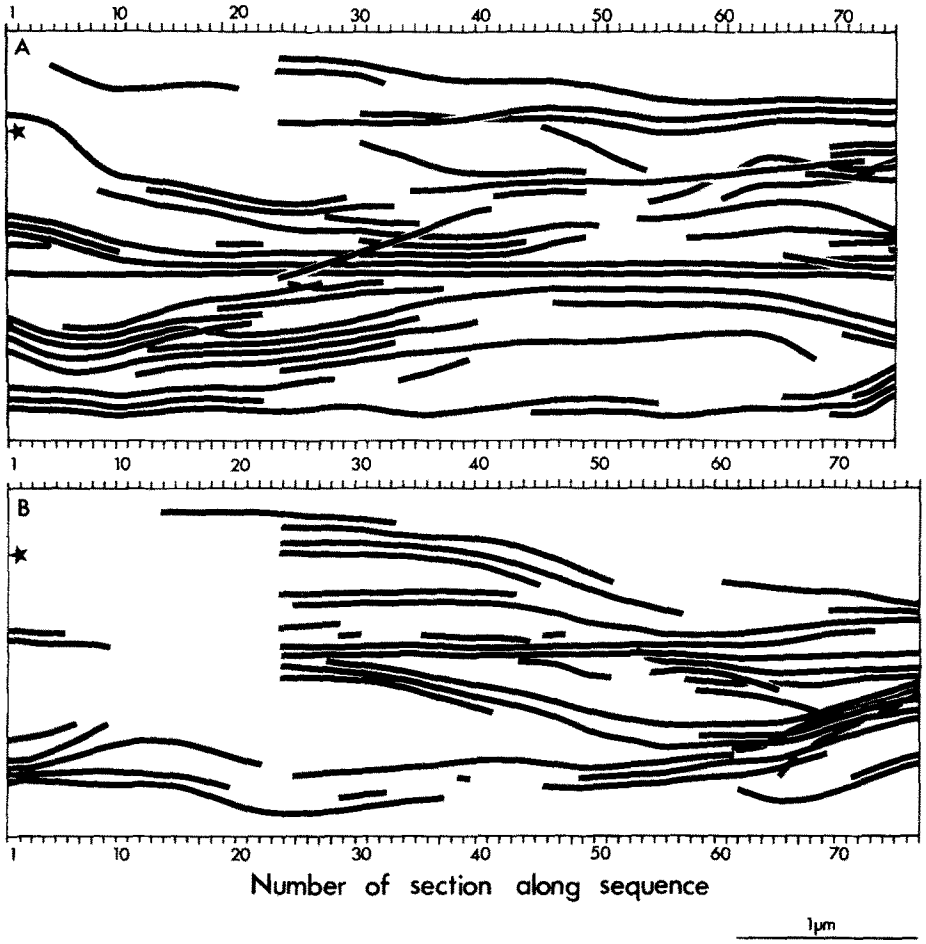

FIGURE 6 Scale representations of two arrays of cortical microtubules against the longitudinal cell walls at interphase. The view in Fig. 6 A is as from the center of the cell, looking outwards. Fig. 6 B represents the cortex of the neighboring cell, viewed by looking on through Fig. 6 A and the intervening wall. The two arrays can be superimposed in register by using the left-hand frame and the asterisks as reference marks. The axis in which the cells were elongating runs up and down the page. *Azolla pinnata*.

part of the work, the distribution of microtubule terminations showed some form of nonrandomness.

The Average Length of Microtubules

The sequences of serial sections and the maps drawn from them show that the observed microtubule lengths range widely from microtubules which are recognizable in only one section up to the longest microtubule so far detected, which was still continuing after 84 sections (5.9 μm). Despite the variation in length, semiquantitation is possible. There are two terminations for each microtubule in an array when the total thickness of the combined serial sections (a) just matches the average microtubule length (L). Sequences of sections that are shorter or longer than this will contain correspondingly fewer or more terminations:

$$\frac{\text{no. of terminations in sequence } (T)}{2 \times \text{average number of microtubules per section } (N)} = \frac{a}{L}.$$

A more rigorous derivation of this formula is set out in Materials and Methods. Strictly, it should only be used where the distribution of terminations conforms to a poisson distribution. The data

have, however, been pooled because the nonrandom arrays were not obviously different from the random in terms of calculated average length. In calculating microtubule lengths, it was assumed that all microtubules lay at right angles to the plane of section and that the cell cortex was flat rather than curved: both assumptions lead to slight underestimation of true lengths.

STANDARD FIXATION PROCEDURE: The data from the sequences of serial sections through arrays of cortical microtubules in *Azolla pinnata* root tip cells and the calculated average lengths are shown in Table I. There is considerable deviation from the mean in each category, but the average lengths, in general, are ~2–4 μm, irrespective of the type of array. Values of 3–4 μm were obtained for *Zea mays* and 5–6 μm for *Impatiens balsamina* (Table II). In all three plants, the average microtubule length was approximately one-eighth of the circumference of the cells that were examined.

ALTERNATIVE FIXATION PROCEDURES: The duration of glutaraldehyde prefixation (see Table I) was varied when preparing the material described in the preceding section, and it was clear that these variations had no major effect on the results. *Azolla* root tips were also fixed in 2.5% glutaraldehyde in a polymerization medium containing 1 mM guanosine triphosphate (GTP), 1 mM magnesium sulphate, 2 mM ethylene glycol-bis(β-aminoethyl ether)*N,N'*-tetraacetic acid and 100 mM piperazine-*N,N'*-bis[2-ethane sulphonic acid] buffer, pH 6.9. In other experiments the GTP was omitted. The general ultrastructure of the cells, and more specifically, of the microtubule arrays, did not differ from that seen after conventional fixation in phosphate-buffered glutaraldehyde. A reconstruction of an interphase array in tissue fixed in the complete polymerization medium is shown in Fig. 7. The average microtubule lengths (Table III) were slightly longer than in conventionally prepared roots, but the difference is not significant. Fixation of roots in polymerization medium lacking GTP made no significant difference with respect to the average microtubule length. None of the 181 terminations observed after fixation in polymerization medium was C-shaped (Table V).

A root fixed in polymerization medium provided another example of abrupt changes in the numbers of microtubules per section due to the presence of lines of terminations. The 16-section sequence cut through an initially highly stacked pre-prophase band (Fig. 8). Three bands of terminations are evident, all parallel to the plane of sectioning and giving rise overall to significant deviation from the poisson distribution. The microtubule terminations in the other sequences of

TABLE I

Average Lengths of Cortical Microtubules in Azolla Root Tip Cells

Type of microtubule array	No. of sections in sequence (×0.07 = a, μm)	Average no. of microtubules per section (*N*)	No. of terminations in sequence (*T*)		Calculated average microtubule length (*L*)
					μm
At xylem thickenings	9*	6	2		4.0
	9*	9	4		2.8
	9*	9	7		1.7
	9*	13	10		1.7
	12*	14	12		1.9
	12*	16	8		3.4
				mean	2.5 ± 0.97
Pre-prophase band	41*	16	28		3.2
	21‡	37	44		2.4
	22‡	51	80		2.0
	33§	47	109		2.0
				mean	2.4 ± 0.57
Interphase	14§	11	5		4.2
	14§	11	4		5.5
	20‖	9	9		2.7
	12*	15	9		2.9
	23§	8	16		1.7
	23§	11	19		1.8
	20‖	19	28		1.9
	50‖	10	29		2.4
	50‖	11	24		3.8
	76¶	10	57		1.9
	30**	27	22		5.1
	74¶	16	66		2.5
	40*	30	42		3.8
	90**	16	72		2.9
				mean	3.1 ± 1.23

Each line in the table represents a different sequence of serial sections. The first three columns of data give the quantities needed to calculate the average microtubule length (*L*) using the formula $L = 2Na/T$. Individual and mean values for each category of microtubule array are given in the last column.

Duration of fixation in glutaraldehyde:

* 4 h.

‡ 8 h.

§ 10–15 min.

‖ 2 h.

¶ 6 h.

** 17 h.

TABLE II

Average Lengths of Cortical Microtubules in Zea and Impatiens Root Tip Cells

Species	Type of microtubule array	No. of sections in sequence	Average no. of microtubules per section	No. of terminations in sequence	Calculated average microtubule length
					μm
Zea mays	Pre-prophase band	22	41	44	2.8
	Interphase	18	10	10	2.6
		18	14	8	4.7
		18	18	12	3.8
				mean	3.7 ± 1.05
Impatiens balsamina	Interphase	30	11	10	4.4
		19	25	12	5.4
		24	20	10	6.9
				mean	5.6 ± 1.26

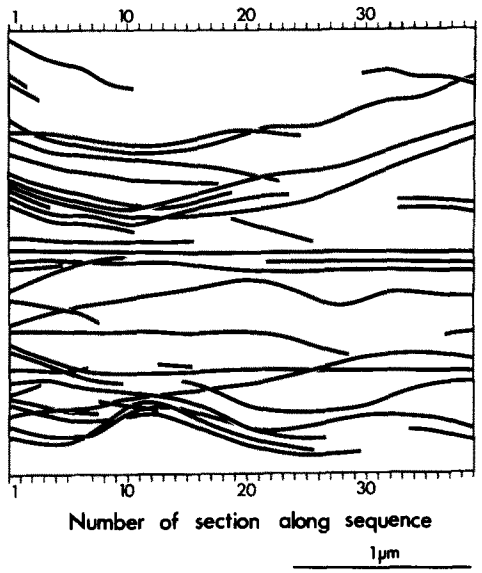

FIGURE 7 An interphase array of microtubules in a root fixed in glutaraldehyde dissolved in complete polymerization medium (see text).

sections of material fixed in this way were randomly distributed according to both poisson and pattern analyses.

Complete Microtubules

Many of the sequences of serial sections included some complete microtubules. Table IV lists the numbers of complete microtubules in four length categories, expressed in each case as a percentage of the total number of microtubules present in the sequence. Because terminations have been arbitrarily taken to occur halfway through the section, the complete lengths cited in the table are one section thickness less than the combined thickness of the sections in which the microtubule was seen. The table includes only complete microtubules up to 1.4 μm in length, although longer ones did occur in the longer sequences. The advantage of expressing the numbers of complete microtubules in this way is that sequences of similar total thickness can be compared. For example, in a comparison of conventional fixation versus fixation in polymerization medium, no differences emerge. On the other hand, some of the treatments to be described below had marked effects on the length distribution of the microtubules.

Treatments Which Can Cause Depolymerization of Microtubules

LOW TEMPERATURE: The cold treatments employed in this work did not lead to the complete disappearance of microtubule arrays in the root tip cells. 22.4% of all terminations found in material fixed in the cold without any recovery time were C-shaped—13 times the frequency seen in control tissues. In one sequence of sections, two C-shaped terminations pointed in one direction and 10 in the other; in another sequence, two pointed one way and 1 the other. The distribution of terminations was random in two sequences, but the one illustrated in Fig. 9 was nonrandom according to the poisson and the pattern analyses. Calculation of average lengths (Table VI A) reveals a diminution to about half that found in controls, and a rapid (15 min) recovery to the normal range of lengths. The proportion of short microtubules was only slightly greater than in controls (Table IV B).

TABLE III

Average Lengths of Cortical Microtubules in Azolla after Fixation in a Microtubule-Polymerization Medium

Treatment	Type of microtubule array	No. of sections in sequence	Average no. of microtubules per section	No. of terminations in sequence	Calculated average microtubule length
					μm
Complete polymerization medium	At xylem thickenings	19	17	14	3.2
	Pre-prophase band	16	46	98	1.0
	Interphase	6	11	4	2.2
		8	10	4	2.7
		6	15	4	3.2
		14	8	2	7.5
		8	18	4	5.0
		8	19	9	2.4
		21	11	7	4.5
		39	19	35	3.0
				mean	3.8 ± 1.8
Polymerization medium minus GTP	Interphase	8	12	6	2.2
		13	8	7	2.1
		10	18	4	6.2
		13	22	5	2.7
				mean	3.3 ± 1.95

HIGH PRESSURE: The effect of high pressure is not straightforward. After a 30-min treatment at 6,000 lb/in^2, the average length was 5.2 μm (Table VI B), yet after 2 h recovery, the value obtained was 1.5 μm. Longer sequences and higher pressures gave more consistent data, 15 min at either 14,000 or 16,000 lb/in^2 reduced the average length to less than half of that seen in controls (Table VI B).

A reconstruction of a 55-section sequence of a pre-prophase band in a root fixed immediately after 15 min at 14,000 lb/in^2 is shown in Fig. 10. Both poisson and pattern analyses indicate that the terminations are nonrandomly distributed. The proportion of short complete microtubules is large (Table IV B), 28% being <0.35 μm in length, compared with 14 and 0% in this size class in two 50-section sequences in controls. A 33-section sequence after 16,000 lb/in^2 treatment also had augmented numbers of short microtubules. The proportion of C-shaped terminations was as in controls, and only one sequence had more than one present. In it, both C-shapes pointed in the same direction.

COLCHICINE: Microtubules were present in some *Azolla* root tip cells even after 2–5 h in 5 × 10^{-3} M colchicine solution. 3.6% of their terminations were C-shaped (Table V). Two sequences had two C-shapes, and in each the two C-shapes pointed in opposite directions. The percentage of short complete microtubules was raised relative to the controls (Table IV B), and the average microtubule lengths were approximately one-third to one-half those in untreated roots, even after a 1-h recovery period (Table VI C). In three of the six sequences, the microtubule terminations were nonrandomly distributed.

Treatment with D_2O

Exposure of *Azolla* roots to D_2O for 5 h produced microtubule arrays which contained large numbers of short microtubules (Table IV C and Fig. 11). The average microtubule length was approximately half that in controls (Table VII). The frequency of C-shaped terminations was 0.9%. Only one sequence contained more than one, and in it, all three C-shapes pointed in the same direction. As illustrated in Fig. 4 B, short microtubules appear in response to D_2O treatment amongst those that are found over developing xylem thickenings; microtubules may in addition be initiated between the thickenings, where their frequency would normally be low (cf. Fig. 4 A). After 18 h in D_2O, the average length was nearly that in controls (Table VII), as was the length distribution (Table IV C); the frequency of C-shaped terminations was zero (Table V).

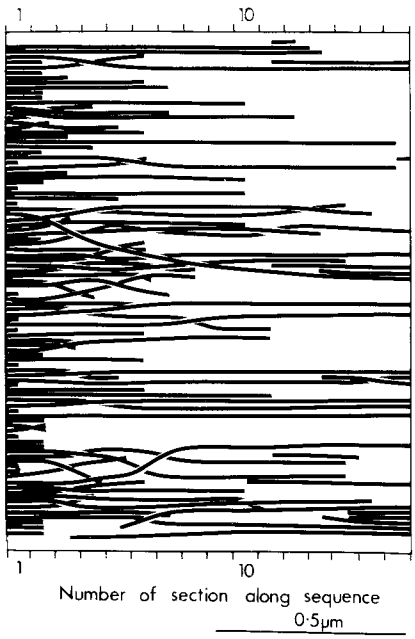

FIGURE 8 A pre-prophase array in a root fixed in glutaraldehyde dissolved in complete polymerization medium. Due to the complexity of this array, the mapping process has in this case involved spacing the microtubules along the plasma membrane and also straightening out their undulations.

DISCUSSION

The major result reported here is that most cortical microtubules in plant cells are short relative to the dimensions of the cell circumference. Microtubule arrays may extend over large or restricted expanses of cell cortex, but the continuity of an array is merely statistical, the constituent microtubules being present as overlapping units of varying but limited length, on average one cross-sectional profile in every 18 representing a terminating microtubule. Before discussing the implications of this observation, the validity of the methods used must be examined.

Methods

No direct check on the efficacy of glutaraldehyde fixation with respect to cortical microtubules has yet been devised. Attempts to use polarized light microscopy as a nondestructive method to assess microtubule densities *in vivo*, followed by comparison with counts made after fixation, would not be suitable for the plant cell cortex where any birefringence due to the microtubules would be masked by that of the cell wall. Glutaraldehyde does, however, fix microtubules that have been polymerized *in vitro*, and affords protection from alterations to their length (31). It also preserves rings, sheets, and tubules in the same proportions as observed in negatively stained preparations of polymerizing mixtures, and it prevents free tubulin from polymerizing (25).

It was found that the duration of the glutaraldehyde fixation step can be altered between 10 min and 17 h with no marked effects upon microtubule length (Table I). Dispositions that might be interpreted as being due to an originally intact microtubule fracturing and the ends so formed moving apart are rare in the reconstructions: one example is in section 41 of Fig. 6 A. The existence of cell-specific features in the back-to-back arrays of Fig. 6 A and B also argues against major mechanical damage during specimen processing. Reports (30, 31) that relatively slow entry of glutaraldehyde permits the buffer to alter the degree of polymerization of tubulin within HeLa cells appeared in the course of the present work. In *Azolla* roots, unlike HeLa cells, the microtubule lengths are essentially the same whether the glutaraldehyde is dissolved in phosphate buffer or in polymerization medium with or without GTP.

If microtubules longer than those detected by the tracking procedure were consistently found in planes of section that show their longitudinal aspect, then doubt would be cast on the methods used here. In fact, the longest segment of cortical microtubule found in a collection of several thousand micrographs of *Azolla* root tips measured 2.5 μm, despite the use of thick sections (0.2–0.5 μm) and high voltage electron microscopy in part of the work to search for longer profiles. All papers on cortical microtubules listed in a recent review (21) have been inspected, and again, no microtubules longer than 1–2 μm were found in the published micrographs, with the exception of two examples, at 3.9 and 3.6 μm, in freeze-fractured pea root tip cells (36). Longer profiles would be expected in freeze-fractured material, as a fracture plane can follow a curved cell cortex whereas a planar ultrathin section cannot. There may, however, be an additional factor, for the pea roots in question were soaked, without prefixation, for 1–10 days in 20% glycerol. Glycerol is now known to support polymerization of tubulin (49), binding to and allowing otherwise inactive tubulin to assemble into microtubules (9). Thus, there is no conflict between the longitudinal views

TABLE IV

Percentages of Complete Microtubules in Cortical Microtubule Arrays in Azolla Root Tip Cells

Treatment	Type of microtubule Array	No. of sections in sequence	Total no. of microtubules	Complete microtubules, as % of total no., in different length classes (μm): 0–0.35	0.42–0.7	0.77–1.05	1.12–1.4
A. Glutaraldehyde in 0.025 M phosphate	Interphase	90	52	2	2	2	2
		76	39	13	10	0	8
		74	51	2	12	2	8
		50	24	14	4		
		50	27	0	4	4	
	Pre-prophase	41	32	3			
	Interphase	40	52	4	2		
	Pre-prophase	33	109	0	6	4	1
	Interphase	30	38	0	3		
	Pre-prophase	22	95	2	2		
		21	58	7	3	2	
	Interphase	20	33	6	3		
		20	14				
Glutaraldehyde in complete polymerization medium	Interphase	39	41	2	5		
		21	14	7			
B. Low temperature							
0°C, 15 min	Interphase	31	40	8	5	5	
1.6°C, 4 h		26	18	4	0	4	4
2°C, 15 min + 15 min recovery		22	27	0	0	5	
High pressure:							
14,000 lb/in²	Pre-prophase	55	71	28	6	4	3
16,000 lb/in²	Interphase	33	25	16	4	8	
Colchicine							
2 h	Interphase	19	48	15	14		
2 h		29	19	0	11	11	
3 h		39	26	4	4		
5 h		31	27	11	8	4	
2 h + 1 h recovery		18	31	16	3		
C. Deuterium oxide							
5 h	Xylem	29	38	13			
	Pre-prophase	50	194	25	13	7	3
	Interphase	56	66	23	14	2	
18 h		34	27	7			
		35	23	4	4		

and the results obtained by tracking, and this, together with the ability to detect interspecific and intertreatment differences in microtubule lengths, gives added confidence that the fixation and tracking procedures used here are valid, at least for the relatively simple arrays found in the plant cell cortex.

Arrays of Overlapping Constituent Microtubules

Cortical arrays in plant cells are not the only examples of systems composed of overlapping microtubules. They occur in myogenic cells (59) and in a variety of mitotic spindles: in nonkinetochore fibres in *Haemanthus* endosperm (23, 26); in an insect spermatocyte (11), where <1% of the tubules were traced and lengths in the range of 1.0–5.5 μm found; in mammalian cells in tissue culture (32, 33); and in the fungi *Thraustotheca* (18) and *Uromyces* (20). The formulae used in the present work can be applied to two of the published sets of data. In myogenic cells (59), data for one set of serial sections yield a calculated average microtubule length of 27 μm in a cell ~150 μm long, with the distribution of the observed terminations conforming to a poisson dis-

tribution. In *Uromyces* (20) a 22-section sequence contained complete microtubules between 1 and 15 section thicknesses in length, and the formula gives an average length of 2 μm.

That cortical arrays of microtubules in plant cells consist of overlapping microtubules provides an explanation for the disparity in numbers that has sometimes been recorded for different parts of the same array, in wheat[1] and *Azolla* (present work) root tip cells, cells of *Sphagnum* "leaflets" (46–48), in hypocotyl cells (45) and in the protonema of a fern (58). In both *Azolla*[2] and *Sphagnum* (48), the numbers are greater along the younger wall. Such occurrences would not be possible if the microtubules were in the form of continuous hoops or spirals, and their implication is that the density of the array alters across the face of the cell, much as mapped in Figs. 5 and 8. In at least some cases, particularly in pre-prophase bands, it is very probable that the density differences arise because the development of the array is incomplete or because it is breaking down progressively from one side of the cell. The lengths of the complete microtubules in the sequences of sections varied widely, and it is important to know whether there might be a proportion of very long representatives, which might approach the dimensions of the "hoops" that are referred to so often in the current literature (see the introduction).

The points that are plotted in Fig. 12 represent, for each sequence of serial sections, the number of microtubules that passed right through the sequence with neither termination included, normalized by expressing it as a fraction of the average microtubule number in the array; this fraction is plotted against the number of sections in the sequence. The value of the fraction approaches unity as the number of sections per sequence is reduced, and diminishes as the number of sections increases, reaching zero in two of the longest sequences. Values for all fixation regimes and all categories of microtubule array in roots that had not been subjected to experimental treatment were pooled before using the least squares method to fit the exponential decay curve shown in Fig. 12. The results may be interpreted as showing an exponentially decreasing probability of finding microtubules of length equal to or greater than the combined section thicknesses, as the number of sections per sequence is increased. Extrapolation of the curve of best fit suggests that if it were possible in practice to follow the whole circumference of a 10-μm diameter cell by serial sectioning, the probability of finding a microtubule of length equal to the total circumference would be 8×10^{-6}. The available data thus point strongly to the absence of microtubules of length comparable to the cell circumference.

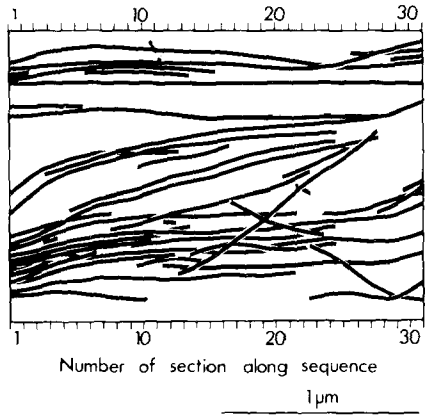

FIGURE 9 A pre-prophase band of microtubules in an *Azolla* root fixed after 15 min at 0°C. This treatment has resulted in an overall decrease in microtubule length.

Perturbations of the Arrays

The data on treatments which in other systems alter the stability of the tubulin:microtubule equilibrium in favor of either assembly or disassembly are limited because the sample sizes obtained through the use of serial sectioning are extremely small. Further, particularly in the case of the depolymerizing treatments, the sequences of sections are highly selected because the majority of cells had lost a considerable proportion of their cortical microtubules. It is not known whether such losses might be selective, as in other systems (3, 44). The maps (Figs. 9 and 10) and data (Tables IV B and VI) presented here therefore represent either surviving or recovering areas of cell cortex, examined in the hope that the form of the microtubules might give some insights into the dynamics of the arrays.

The depolymerizing treatments fall into two categories, though all three reduced the average length (Table VI). Colchicine and high pressures gave rise to arrays with greatly augmented proportions of short microtubules (Table IV) without,

[1] O'Brien and Maynard. Personal communication.

[2] A. R. Hardham and B. E. S. Gunning. Manuscript in preparation.

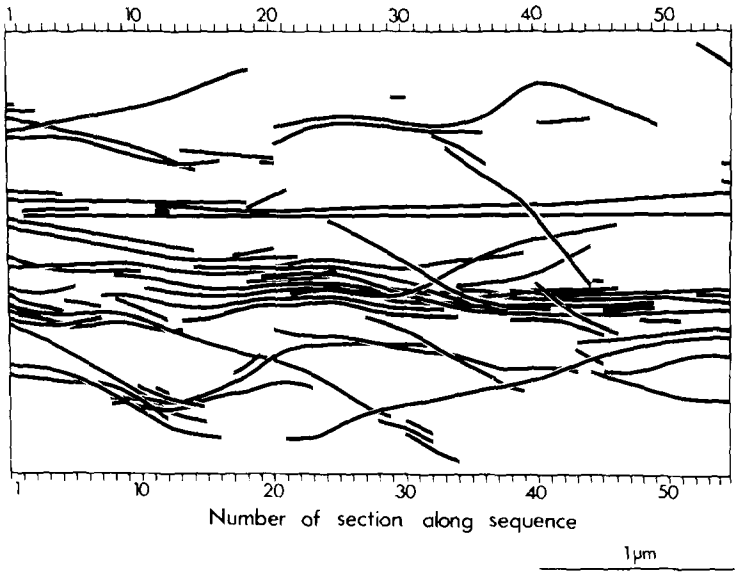

FIGURE 10 A pre-prophase band of microtubules in an *Azolla* root subjected to a pressure of 14,000 lb/in^2 for 15 min. The array contains a large number of very short microtubules, 34% being <0.7 μm in length, approximately three times the frequency seen in sequences of comparable length in untreated roots.

TABLE V
Percentages of C-Shaped Terminations

Treatment	Total no. of terminations observed	Percent of C-shaped terminations
Control	706	1.7
Polymerization medium	181	0
Low temperature	67	22.4
High pressure	234	1.7
Colchicine	139	3.6
5 h D_2O	445	0.9
18 h D_2O	87	0

however, producing large increases in the proportion of C-shaped terminations (Table V). Low temperature, on the other hand, had little effect on the length distribution, but produced very high frequencies of C-shapes. In this latter case, an interpretation that is consistent with the data is that the microtubules had (on average) shortened through terminal disassembly, many of them opening out to give the C-profile; the shortest microtubules initially present had disappeared and were replaced by remnants of longer ones, the average length thus falling. It is not ruled out, however, that some C-shapes might be generated in the cold without accompanying disassembly. The former pattern, induced by colchicine and high pressure, is suggestive of fragmentation, presumably in addition to disassembly, or, alternatively, of early stages in recovery when the population contained short but growing microtubules.

In general, D_2O is reported to stabilize microtubule arrays and enchance microtubule formation from available pools of tubulin (22, 54). In plants, no effects were found in wheat root tips (6) and rye leaves (57), yet in *Sphagnum* leaf cells at the same stage of the cell cycle there was a 25% increase in the number of microtubules (48). For pre-prophase bands, a marked increase in microtubule numbers was claimed for wheat roots (6), yet in *Sphagnum* the band appeared more transient and indistinct (48). Observations of pre-prophase bands in untreated *Azolla* roots[3] show great variation in microtubule numbers, presumably reflecting developmental changes, and the map shown in Fig. 8 serves to emphasize that the number of microtubules per section can be a poor criterion for this type of experiment. More reliance can, however, be placed on observations of microtubule length within a given array. A 5-h treatment in D_2O skewed the length distribution strongly towards short microtubules as compared

[3] B. E. S. Gunning, A. R. Hardham, and J. E. Hughes. Manuscript in preparation.

with controls (Table IV). This applied to all three categories of array, and a likely interpretation is that additional tubules were generated which, being short, lowered the overall average length (Table VII). There was no general diminution in microtubule numbers throughout the root tip such as was observed in the depolymerizing treatments. After 18-h treatment, the length distribution and the average length approximated to the control situation, and in the absence of firm information on total numbers per cell or per unit length of wall, the only valid interpretation of this seeming return to normality is that the response to D_2O does not involve enhancement of assembly onto existing microtubules (which would have increased the average length), but rather the gener-

TABLE VI

Average Lengths of Cortical Microtubules in Azolla Root Tip Cells after Depolymerization Treatments

Treatment	Type of microtubule array	No. of sections in sequence	Average no. of microtubules per section	No. of terminations in sequence	Calculated average microtubule length
					μm
A. Low temperature					
0°C, 15 min	Interphase	31	19	48	1.7
1.6°C, 4 h		26	8	19	1.5
2°C, 15 min + 15 min recovery		22	17	18	2.8
B. High pressure					
6,000 lb/in², 30 min	Interphase	14	21	8	5.2
6,000 lb/in², 30 min + 2 h recovery	Pre-prophase	14	74	95	1.5
14,000 lb/in², 15 min		55	17	108	1.2
16,000 lb/in², 15 min	Interphase	33	9	31	1.3
C. Colchicine					
2 h	Interphase	19	15	53	0.8
		29	11	20	1.9
2 h + 1 h recovery		18	8	36	0.6
3 h		39	14	25	1.2
5 h		31	6	33	0.8

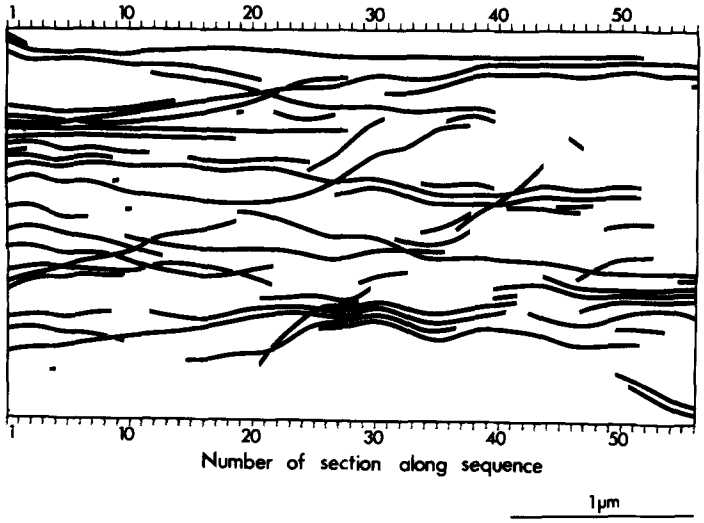

FIGURE 11 An interphase array of microtubules in an *Azolla* root which had been immersed in D_2O for 5 h. Dispersed throughout the array is a large number of short microtubules, the presence of which lowers the calculated average microtubule length.

TABLE VII

Average Lengths of Cortical Microtubules in Azolla Root Tip Cells after Deuterium Oxide Treatment

Treatment	Type of microtubule array	No. of sections in sequence	Average no. of microtubules per section	No. of terminations in sequence	Calculated average microtubule length
					μm
5 h D_2O	Xylem	11	7	15	0.7
		13	16	17	1.7
		29	15	38	1.7
	Pre-prophase	50	50	293	1.3
	Interphase	13	9	21	0.8
		10	21	14	2.1
		56	16	96	1.3
18 h D_2O	Pre-prophase	8	46	24	2.2
	Interphase	13	10	7	2.7
		13	15	14	1.9
		12	20	11	3.1
		35	13	19	3.2
		34	16	22	3.4

ation of new ones.

Treatments which should favor polymerization (presence of GTP, D_2O) diminished the proportion of terminations with C-shapes, whereas low temperature and (to a lesser extent) colchicine increased this proportion. It has been claimed that the C-shape is associated with disassembly (43), but it can also occur at growing terminations *in vivo* (1) and *in vitro* (5) (for full discussion see references 7, 23, and 26). C-shaped profiles were not restricted to the ends of the microtubules, even in untreated material, and low temperatures enhanced the proportion of subterminal C-shapes.

Of the 325 complete microtubules that were mapped, 15 had a visible manifestation of polarity, *viz.*, a C-shaped profile at one end but not at the other. No microtubules with C-shapes at both ends were found. An obvious interpretation of this morphological polarity is that the microtubules grow or disassemble preferentially at one end, as has been observed *in vitro* (see references 8 and 51). It is therefore of great interest that C-shapes are patterned in the microtubule maps. When serial sections are examined, the C-shapes point in the same direction. The observed numbers of C-shapes were as follows (expressed in the form of the number of C-shapes pointing one way:number pointing the opposite way) 0:2, 0:4, 0:6 (controls); 0:3 (5 h, D_2O); 0:2 (high pressure); 2:10, 1:2 (low temperature); and 1:1, 1:1 (colchicine). The observations on colchicine-affected arrays are few, but suggest that the microtubules in them, although still polar as individuals, do not share a common polarity. In the controls and D_2O treatment, at least those microtubules that have C-shaped terminations share a common morphological directionality. It is not known whether this sharing extends to the majority of the microtubules (those lacking C-shaped terminations), nor is it known whether all faces, or indeed all parts of faces, of a cell share the same directionality. The cell cortex could be subdivided into domains that differ from one another but within which directionality is shared.

Development of Cortical Arrays

In undertaking the present work, one expectation was that evidence for microtubule-organizing structures might emerge. In fact, the great majority of microtubule terminations are not patterned, with the exception of some clustering (e.g. Fig. 2 in reference 17). Precedents for linear microtubule-organizing centers (MTOCs) which generate microtubules at right angles to their long axis do exist in the algae (2, 4), but no ultrastructural evidence for any equivalent of these rhizoplast fibers was found here. The lines of terminations may well be significant, particularly the two that lay back-to-back in neighboring cells, in or close to the direction of cell elongation (Fig. 6). They can, however, hardly be indicative of MTOCs unless these are so few in number that the sample sequences of sections rarely included them, or unless some form of propagation and turnover of the population of microtubules obliterates a patterned origin that is conspicuous only transiently in an earlier stage of the cell cycle. It must be emphasized that the sample sizes are not only

small relative to the surface area of the cell, but also selective: because of the practical problems of tracking microtubules, they did not penetrate into any cell corners, which therefore remain as possible sites for MTOCs.

The majority of cortical microtubules, short or long, lie parallel to and at varying distances from the plasma membrane, this being especially evident in highly stacked pre-prophase bands. Detailed examination of the serial sections shows that microtubules, even very short ones, do not bend towards and terminate "in or on the plasma membrane," as suggested for *Allium* root tip pre-prophase bands (37). The source and mechanism of placement of any initiator molecules that may be required (see references 5 and 51) are therefore unknown. It should be pointed out that the microtubules are not necessarily assembled where they are seen. Neither the literature nor the present results preclude the concept of an assembly process that is followed by mobility of microtubules within the arrays. Once initiated, the ultimate length of the microtubules could be governed by the balance between the numbers of free tubulin molecules and the numbers of competing assembly sites, as demonstrated *in vitro* in experiments where a given quantity of tubulin can be used to make many short microtubules or fewer longer ones (5, 50). Further experiments with D_2O, which, as described above, seem to induce additional microtubules rather than elongate existing ones, might be helpful in this context.

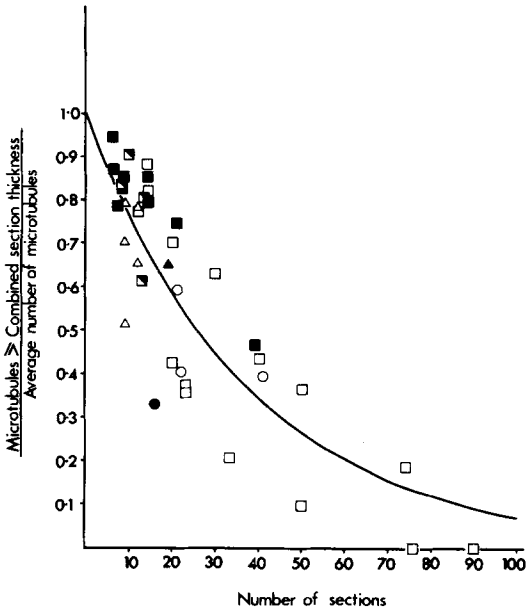

FIGURE 12 The fraction of microtubules in an array which pass right through the sequence of sections, plotted against the number of sections in the sequence. Squares, interphase arrays; circles, pre-prophase bands; triangles, arrays overlying xylem thickenings. Open symbols, conventional fixation; closed symbols, fixation in polymerization medium + GTP; half-closed squares, fixation in polymerization medium without GTP. The curve was fitted by the least squares method and represents the relationship $y = e^{-0.0265s}$, where y is the ordinate and s is the number of sections in a sequence.

Some estimates of microtubule growth rates are available. In plant material, microtubule growth keeps pace with the 1–2 μm min^{-1} elongation rate of root hairs (35). Values up to 1.4 μm min^{-1} for *in vitro* growth are reported, dependent upon the tubulin concentration and the concentration of polyanion (5). The rate of 1.5 μm min^{-1} claimed for reassembling mitotic spindles (12) may be an overestimate in that it rests on the assumption that the spindle fibers, which were measured by optical microscopy, consist of continuous rather than overlapping microtubules, with single rather than multiple growing points. The *Azolla* roots used here were elongating, and unpublished data on the interpolation of additional microtubules along the cell walls suggest that their growth rates approach the above values. It is not known whether, or how, turnover of the components of cortical microtubule arrays is accomplished. At one extreme, entire microtubules could disassemble and be replaced at the growth rates suggested above, in which case the lifetime of a 2–4 μm long microtubule might be only a few minutes. The low frequency (1.7%) of C-shaped terminations militates against this view. Alternatively, individual microtubules, once formed, might be stabilized by becoming cross-bridged to adjacent structures.

Bridges occur between adjacent microtubules and between microtubules and membranes in *Azolla*, as in other plant cells (21). The present observation of periodic cross bridging in arrays of plant cortical microtubules is of potential significance with respect to possible functions, be they in microtubule assembly, in stabilizing and orienting the microtubules, in stabilizing domains or molecules in or on the plasma membrane, or in mediating motility phenomena. We are grateful to Dr. P. B. Green (Stanford University, Stanford, Calif.) for pointing out to us that, in arrays of overlapping component microtubules such as

we have detected, mechanochemical interactions which tend to maximize the extent of overlap will influence the overall orientation. In the case of the side walls of approximately cyclindrical cells such as examined here, maximization of overlaps would hold the constituent microtubules under tension, the array as a whole becoming predominantly transversely oriented.

Microtubules and Microfibrils

Much of the preceding discussion has centered on the properties of the extensive microtubule arrays that lie against the longitudinal walls of elongating *Azolla* root tip cells, where the microtubules and the cellulose microfibrils[4] share a predominantly transverse orientation, just as in other species. However, deposition of cellulose can also be precisely localized in small areas of the cell surface, as at pits (42) or the thickenings of stomatal pores (38). Whereas it is difficult to envisage how arrays of long "hooplike" microtubules could be locally differentiated in order to participate in such events, the present observation that cortical arrays consist of short overlapping components does at least allow the concept of microtubule participation to be applied to both large and small expanses of wall: the only difference in principle is the degree to which the array of overlapping microtubules is propagated around the cell cortex. At both pits (42) and stomatal pores (38) the microtubules and wall microfibrils are co-aligned, which confronts us once again with the major problems of how microtubule arrays become localized and oriented. It may be that the systems that control the formation of extensive as compared to spatially restricted arrays are considerably different.

The observations presented here have no direct bearing on the possible role of cortical microtubules in orienting the deposition of cellulose microfibrils. However, the view that the cortical microtubules represent "relatively rigid tracks along which other cellular components (such as cellulose synthetase complexes projecting inwards through the plasma membrane to the microtubules) might move" (19) is now unattractive because the "tracks" are seen to be too short. Guidance of cellulose synthetase complexes by means of microtubule movements generated by intertubule sliding or polarized assembly-disassembly is not ruled out, nor is indirect guidance by the production of shearing forces in the membrane by motility-generating molecules associated with the cortical microtubules (21). Indeed, the latter suggestions receive a measure of support from the detection of polarity in the cortical arrays.

[4] Polarized light microscope observations by Dr. P. B. Green, Stanford University, personal communication.

We thank Drs. D. J. Carr, P. B. Green, P. K. Hepler, and E. H. Newcomb for valuable discussions in the course of the work and the preparation of the manuscript. The hospitality and help given to B. E. S. Gunning in the High Voltage Electron Microscopy Laboratory in the Department of Molecular, Cellular and Developmental Biology in the University of Colorado, Boulder, is gratefully acknowledged.

Received for publication 8 September 1977, and in revised form 2 December 1977.

REFERENCES

1. Behnke, O. 1967. Incomplete microtubules observed in mammalian blood platelets during microtubule polymerization. *J. Cell Biol.* **34**:697–701.
2. Bouck, G. B., and D. L. Brown. 1973. Microtubule biogenesis and cell shape in *Ochromonas*. I. The distribution of cytoplasmic and mitotic microtubules. *J. Cell Biol.* **56**:340–359.
3. Brinkley, B. R., and J. Cartwright, Jr. 1975. Cold-labile and cold-stable microtubules in the mitotic spindle of mammalian cells. *In* The Biology of Cytoplasmic Microtubules. D. Soifer, editor. *Ann. N. Y. Acad. Sci.* **253**:428–439.
4. Brown, D. L., and G. B. Bouck. 1973. Microtubule biogenesis and cell shape in *Ochromonas*. II. The role of nucleating sites in shape development. *J. Cell Biol.* **56**:360–378.
5. Bryan, J. 1976. A quantitative analysis of microtubule elongation. *J. Cell Biol.* **71**:749–767.
6. Burgess, J., and D. H. Northcote. 1969. Action of colchicine and heavy water on the polymerization of microtubules in wheat root meristems. *J. Cell Sci.* **5**:433–451.
7. Cohen, W. D., and T. Gottlieb. 1971. C-microtubules in isolated mitotic spindles. *J. Cell Sci.* **9**:603–619.
8. Dentler, W. L., S. Granett, G. B. Witman, and J. L. Rosenbaum. 1974. Directionality of brain microtubule assembly *in vitro*. *Proc. Natl. Acad. Sci. U. S. A.* **71**:1710–1714.
9. Detrich, H. W., III, S. A. Berkowitz, H. Kim, and R. C. Williams, Jr. 1976. Binding of glycerol by microtubule protein. *Biochem. Biophys. Res. Commun.* **68**:961–968.
10. Fisher, R. A. 1948. Statistical Methods for Research Workers. Oliver and Boyd Ltd., Edinburgh.

11. FUGE, H. 1974. The arrangement of microtubules and the attachment of chromosomes to the spindle during anaphase of Tipulid spermatocytes. *Chromosoma (Berl.)*. **45**:245–260.
12. GOODE, D. 1973. Kinetics of microtubule formation after cold disaggregation of the mitotic apparatus. *J. Mol. Biol.* **80**:531–538.
13. GREEN, P. B., R. O. ERICKSON, and B. A. RICHMOND. 1970. On the physical basis of cell morphogenesis. *Ann. N. Y. Acad. Sci.* **175**:712–731.
14. GREIG-SMITH, P. 1952. The use of random and contiguous quadrats in the study of the structure of plant communities. *Ann. Bot. (Lond.)*. **16**:293–316.
15. GUNNING, B. E. S., and A. R. HARDHAM. 1977. Estimation of the average section thickness in ribbons of ultrathin sections. *J. Microsc.* **109**:337–341.
16. GUNNING, B. E. S., A. R. HARDHAM, and J. E. HUGHES. 1976. Morphogenesis and microtubules in *Azolla* root apices. *J. Cell Biol.* **70**(2, Pt. 2): 56*a*. (Abstr.).
17. HARDHAM, A. R., and B. E. S. GUNNING. 1977. The length and disposition of cortical microtubules in plant cells fixed in glutaraldehyde-osmium tetroxide. *Planta. (Berl.)*. **134**:201–203.
18. HEATH, I. B. 1974. Mitosis in the fungus *Thraustotheca clavata*. *J. Cell Biol.* **60**:204–220.
19. HEATH, I. B. 1974. A unified hypothesis for the role of membrane bound enzyme complexes and microtubules in plant cell wall synthesis. *J. Theor. Biol.* **48**:445–449.
20. HEATH, I. B., and M. C. HEATH. 1976. Ultrastructure of mitosis in the cowpea rust fungus *Uromyces phaseoli* var. *vignae*. *J. Cell Biol.* **70**:592–608.
21. HEPLER, P. K., and B. A. PALEVITZ. 1974. Microtubules and microfilaments. *Annu. Rev. Plant Physiol.* **25**:309–362.
22. INOUÉ, S., and H. RITTER, JR. 1975. Dynamics of mitotic spindle organization and function. *In* Molecules and Cell Movement. S. Inoué and R. E. Stephens, editors. Raven Press, New York. 3–30.
23. JENSEN, C., and A. BAJER, 1973. Spindle dynamics and arrangement of microtubules. *Chromosoma (Berl.)*. **44**:73–89.
24. KERSHAW, K. A. 1973. Quantitative and Dynamic Plant Ecology. Arnold (Edward) (Publishers) Ltd., London.
25. KIRSCHNER, M. W., L. S. HONIG, and R. C. WILLIAMS. 1975. Quantitative electron microscopy of microtubule assembly *in vitro*. *J. Mol. Biol.* **99**:263–276.
26. LAMBERT, A.-M., and A. S. BAJER. 1972. Dynamics of spindle fibres and microtubules during anaphase and phragmoplast formation. *Chromosoma (Berl.)*. **39**:101–144.
27. LEDBETTER, M. C. 1967. The disposition of microtubules in plant cells during interphase and mitosis. *Symp. Int. Soc. Cell Biol.* **6**:55–70.
28. LEDBETTER, M. C., and K. R. PORTER. 1963. A "microtubule" in plant cell fine structure. *J. Cell Biol.* **19**:239–250.
29. LEDBETTER, M. C., and K. R. PORTER. 1970. Introduction to the Fine Structure of Plant Cells. Springer-Verlag, Berlin.
30. LUFTIG, R. B., P. N. MCMILLAN, J. A. WEATHERBEE, and R. R. WEIHING. 1976. Increased visualization of microtubules by an improved fixation procedure. *J. Cell Biol.* **70**(2, Pt. 2):228*a*. (Abstr.).
31. LUFTIG, R. B., P. N. MCMILLAN, J. A. WEATHERBEE, and R. R. WEIHING. 1977. Increased visualization of microtubules by an improved fixation procedure. *J. Histochem. Cytochem.* **25**:175–187.
32. MCINTOSH, J. R., W. Z. CANDE, and J. A. SNYDER. 1975. Structure and physiology of the mammalian mitotic spindle. *In* Molecules and Cell Movement. S. Inoué and R. E. Stephens, editors. Raven Press, New York. 31–76.
33. MCINTOSH, J. R., Z. CANDE, J. SNYDER, and K. VANDERSLICE. 1975. *In* The Biology of Cytoplasmic Microtubules. D. Soifer, editor. *Ann. N. Y. Acad. Sci.* **253**:407–427.
34. NEWCOMB, E. H. 1969. Plant microtubules. *Annu. Rev. Plant Physiol.* **20**:253–288.
35. NEWCOMB, E. H., and H. T. BONNETT, JR. 1965. Cytoplasmic microtubule and wall microfibril orientation in root hairs of radish. *J. Cell Biol.* **27**:575–589.
36. NORTHCOTE, D. H., and D. R. LEWIS. 1968. Freeze-etched surfaces of membranes and organelles in the cells of pea root tips. *J. Cell Sci.* **3**:199–206.
37. PACKARD, M. J., and S. M. STACK. 1976. The preprophase band: possible involvement in the formation of the cell wall. *J. Cell Sci.* **22**:403–411.
38. PALEVITZ, B. A., and P. K. HEPLER. 1976. Cellulose microfibril orientation and cell shaping in developing guard cells of *Allium:* the role of microtubules and ion accumulation. *Planta (Berl.)*. **132**:71–93.
39. PICKETT-HEAPS, J. D. 1966. Incorporation of radioactivity into wheat xylem walls. *Planta (Berl.)*. **71**:1–14.
40. PICKETT-HEAPS, J. D. 1967. The effects of colchicine on the ultrastructure of dividing plant cells, xylem wall differentiation and distribution of cytoplasmic microtubules. *Dev. Biol.* **15**:206–236.
41. PICKETT-HEAPS, J. D. 1974. Plant microtubules. *In* Dynamic Aspects of Plant Ultrastructure. A. W. Robards, editor. McGraw-Hill, New York. 219–255.
42. ROBARDS, A. W., and P. G. HUMPHERSON. 1967. Microtubules and angiosperm bordered pit formation. *Planta (Berl.)*. **77**:233–238.
43. ROTH, L. E., and Y. SHIGENAKA. 1970. Microtubules in the Heliozoan axopodium. II. Rapid deg-

radation by cupric and nickelous ions. *J. Ultrastruct. Res.* **31**:356–374.

44. SALMON, E. D., D. GOODE, T. K. MAUGEL, and D. B. BONAR. 1976. Pressure-induced depolymerization of spindle microtubules. III. Differential stability in HeLa cells. *J. Cell Biol.* **69**:443–454.
45. SAWHNEY, V. K., and L. M. SRIVASTAVA. 1975. Wall fibrils and microtubules in normal and gibberellic-acid-induced growth of lettuce hypocotyl cells. *Can. J. Bot.* **53**:824–835.
46. SCHNEPF, E. 1973. Mikrotubulus-Anordnung und-Umordnung, Wandbildung und Zellmorphogenese in jungen *Sphagnum*-Blättchen. *Protoplasma (Berl.)*. **78**:145–173.
47. SCHNEPF, E. 1974. Microtubules and cell wall formation. *Port. Acta Biol. Ser. A.* **14**:451–462.
48. SCHNEPF, E., G. DEICHGRÄBER, and N. LJUBEŠIĆ. 1976. The effects of colchicine, ethionine and deuterium oxide on microtubules in young *Sphagnum* leaflets. A quantitative study. *Cytobiologie.* **13**:341–353.
49. SHELANSKI, M. L., F. GASKIN, and C. R. CANTOR. 1973. Microtubule assembly in the absence of added nucleotides. *Proc. Natl. Acad. Sci. U. S. A.* **70**:765–768.
50. SLOBODA, R. D., W. L. DENTLER, and J. L. ROSENBAUM. 1976. Microtubule-associated proteins and the stimulation of tubulin assembly *in vitro*. *Biochemistry.* **15**:4497–4505.
51. SNYDER, J. A., and J. R. MCINTOSH. 1976. Biochemistry and physiology of microtubules. *Annu. Rev. Biochem.* **45**:699–720.
52. SPURR, A. R. 1969. A low-viscosity epoxy resin embedding medium for electron microscopy. *J. Ultrastruct. Res.* **26**:31–43.
53. SRIVASTAVA, L. M., and A. P. SINGH. 1972. Certain aspects of xylem differentiation in corn. *Can. J. Bot.* **50**:1795–1804.
54. STEPHENS, R. E. 1973. A thermodynamic analysis of mitotic spindle equilibrium at active metaphase. *J. Cell Biol.* **57**:133–147.
55. THOMPSON, H. R. 1958. The statistical study of plant distribution patterns using a grid of quadrats. *Aust. J. Bot.* **6**:322–342.
56. VENABLE, J. H., and R. COGGESHALL. 1965. A simplified lead citrate stain for use in electron microscopy. *J. Cell. Biol.* **25**:407–408.
57. WABER, J., and W. S. SAKAI. 1975. Further studies of the ultrastructure of D_2O grown winter rye. *Protoplasma. (Berl.)*. **84**:273–281.
58. WADA, M., and T. P. O'BRIEN. 1975. Observations on the structure of the protonema of *Adiantum capillus-veneris* L. undergoing cell division following white-light irradiation. *Planta (Berl.)*. **126**:213–227.
59. WARREN, R. H. 1974. Microtubular organization in elongating myogenic cells. *J. Cell Biol.* **63**:550–566.